Construction and Building Materials 184 (2018) 76–86

Contents lists available at ScienceDirect

Construction and Building Materials

journal homepage: www.elsevier.com/locate/conbuildmat

Optimization of lime and clay-based hemp-concrete wall formulations for a successful lime rendering

A. Arizzi [a,*], M. Brümmer [b], I. Martín-Sánchez [c], E. Molina [d,e], G. Cultrone [a]

[a] Departamento de Mineralogía y Petrología, Universidad de Granada, Avda. Fuentenueva s/n, 18002 Granada, Spain
[b] CANNABRIC, Cañada Ojeda, 8 E-18500 Guadíx, Granada, Spain
[c] Departamento de Microbiología, Universidad de Granada, Avda. Fuentenueva s/n, 18002 Granada, Spain
[d] Centro de Excelencia en Geotermia de los Andes (CEGA, FONDAP-CONICYT), Universidad de Chile, Plaza Ercilla 803, Santiago, Chile
[e] Centro de Investigación en Nanotecnología y Materiales Avanzados, CIEN-UC, Pontificia Universidad Católica de Chile, Avenida Vicuña Mackenna, 4860 Santiago, Chile

HIGHLIGHTS

- Drying time of compacted-hemp concrete blocks is increased by the presence of clay.
- 2-weeks-rendered blocks show more intense pigmentation and microbial colonization.
- Lime putty maintains higher RH underneath the render than natural hydraulic one.
- Aragonite on lime putty render is an evidence of the higher RH and organic content.

ARTICLE INFO

Article history:
Received 30 October 2017
Received in revised form 15 June 2018
Accepted 27 June 2018
Available online 20 July 2018

Keywords:
Hemp
Compacted blocks
Moist conditions
Lime render
Aragonite
Microorganisms

ABSTRACT

Different pathologies may arise on a wall finish if this is applied on a hemp-based rammed wall that is not completely dry. By simulating uneven drying and early-rendering of load-bearing and non-load-bearing hemp concrete blocks (made with natural hydraulic lime only or a mix of lime with clay) and studying them by means of chromatic, microbiological, textural and morphological investigations, we found that: it is advisable to wait at least ten weeks before rendering; adding clay to hemp concrete delays drying, leading to more intense deterioration of the render; natural hydraulic lime is the preferred binder for rendering hemp concrete.

1. Introduction

1.1. Hemp-based building materials

Hemp is a fast-growing, renewable and carbon sequestrating plant [1] that is crop annually for several industrial applications [2], such as food, bio-fuels, packaging, pharmaceutical products, automobiles and building materials [3], among others. To obtain a composite building material made with hemp, the inner part of the hemp stem is cut into pieces or particles (called shiv or hurds) that are mixed with a binder (or a mix of different binders, e.g. lime + cement, lime + clay) and water in different dosages according to the intended function in the building. The resulting product, called hemp concrete, shows high water vapour permeability and flexibility, little shrinkage and is effective in improving thermal and acoustic insulating properties and in regulating relative humidity in the building [4,5].

When in the fresh state (i.e. right after mixing), the hemp-lime concrete can be either moulded or sprayed in conjunction with timber frame for wall insulation and finish, casted in prefabricated panels and blocks to build solid walls or used as infill [4], or even compacted to build rammed earth walls. The fabrication of cast blocks and rammed walls can vary in cost as their composition may differ according to their function as load-bearing or non-load-bearing materials. In the former, indeed, more binder or a small aggregate is added to increase mechanical strength [6]. Besides, cast and rammed hemp concretes show different performances in the building compared to sprayed hemp concretes, as the former are denser and heavier and therefore provide lower thermal insulation [4]. In particular, the hygrothermal properties of hemp concrete change depending on the application process,

* Corresponding author.
E-mail address: arizzina@ugr.es (A. Arizzi).

https://doi.org/10.1016/j.conbuildmat.2018.06.225
0950-0618/

as sprayed concrete lead to faster drying time in comparison to compacted processes; furthermore, intense compaction increases the material density and drying time [7,8]. The drying kinetics of this peculiar material will therefore depend on three main factors: water dosage, application method and exposure conditions (RH, T, solar radiation and wind pressure, providing protection against rainfall).

Estimating the drying time of hemp concrete is fundamental in the view of applying a wall finish, which ideally would be a lime render or plaster. Bevan and Woolley [4] suggested to let cast and rammed hemp concretes dry out for 28 days under normal conditions or 7–10 days (if spray-applied) before the application of a wall finish, but they also recognise that, owing the hygroscopic nature of hemp, hemp concrete cannot be absolutely dry. Colinart et al. [7] also reported that, whatever the formulation (lime, hemp and water dosage) and the drying modes (forced or free convection), the mass of prefabricated blocks is stabilised after approximately 3–4 months since their preparation, at an average RH of 45%. According to their results, ambient conditions are sufficient to cure every type of hemp concrete block and drying can be accelerated by subjecting all the faces to natural convection rather than only one.

1.2. Hemp-based rammed earth walls

Today the inclusion of straw, flax and hemp fibres is increasingly considered as a good method of improving the hygrothermal performances of rammed earth walls [9].

On the basis of the investigations on the drying process of prefabricated hemp concrete blocks commented above, we understand that predicting the drying kinetics of hemp-based rammed earth walls can be an even harder task, especially because environmental conditions are often far from the ideal values and it can be difficult to maintain them constant during construction. Moreover, rammed earth walls are built by compaction method, so drying is slower than in pressed blocks. And also, drying is unlikely to occur evenly in the building, considering that walls have different orientation (i.e. different exposition to sun radiation and wind pressure). As a consequence, it is not unlikely that a protective coating (plaster or render) is applied before the rammed earth wall has completely dried out. In this case, the coating would reduce and delay vapour diffusion [10] and water would be retained longer in the hemp concrete to the detriment of both the wall and the coating performance, especially in relation with its moisture buffering ability [11] and the risk of microbial growth [12], the latter enhanced under moist conditions on materials with organic components (such as hemp concrete) [13]. An example of the pathologies (e.g. yellowish stains and deposition) that are likely to arise in renders and plasters applied on rammed walls made with hemp is shown in Fig. 1.

It is worth highlighting that, although rammed earth walls are often left without any wall finishes, coating is sometimes required to prevent degradation of the surface (in the form of dusting and cracking) due to exposure to wind and rainfall, as well as to improve thermal insulation of the wall [9]. Therefore, the causes of the deterioration forms shown in Fig. 1 need to be understood and prevented to ensure the function of the render or plaster as a protective coating.

In this work we claim to simulate this negative scenario, fabricating hemp-earth blocks with the same method applied for rammed earth walls (by compaction) and letting them dry for a short time before the render application (2 and 10 weeks), through only one surface (the rendered one) and at high relative humidity (RH = 90%) without ventilation. Simulating incomplete drying before rendering at 2 weeks allowed us to investigate the pathologies arisen, by means of chromatic, microbiological, textural and morphological investigations. According to Delgado et al. [13], indeed, this period is the shortest possible time needed for mould growth to start. The same studies were carried out on blocks rendered after 10 weeks of drying, so as to compare the behaviour of wet and dry rendered hemp-earth blocks.

Furthermore, a mineralogical study of the renders was carried out to investigate the outcome of their hardening processes under these conditions. Four types of rammed earth walls made with hemp were reproduced here: load-bearing (with sand) and non-load-bearing ones (without sand) prepared with two different binders (natural hydraulic lime and a mix of natural hydraulic lime with clay). Two types of renders were prepared with lime putty and natural hydraulic lime as binders. Cement render has not been taken into consideration as its use is not recommended for rammed earth walls [9].

The final aim of this study is to estimate an appropriate time for rendering earth walls made with hemp. Furthermore, we aim to understand the influence of the addition of clay to the hemp concrete and of the type of binder used for rendering on the drying behavior of the hemp-earth blocks, with the purpose to improve their durability.

2. Materials and methods

2.1. Raw materials

The components used for the fabrication of the whole blocks (hemp concrete + render) were: natural hydraulic lime (grey

Fig. 1. (a) A house built with rammed hemp concrete walls; (b) pathologies arisen on the plaster of a hemp concrete wall on the inner Northern side of a hemp concrete building (c) detail of the powdered aspect of the yellowish deposition on the same plaster. (For interpretation of the references to colour in this figure legend, the reader is referred to the web version of this article.)

NHL3.5 [14]), produced by Socli, Italcementi Group (Izaourt, France); lime putty (CL90S-PL [14]) stored under water for 4 years, produced by Gordillos Cal de Morón (Seville, Spain); a clayey earth, proceeding from Guadix (Granada, Spain); natural crushed sand of calcitic composition (0.063 < < 3 mm); hemp shiv (2–25 mm long), produced by AgroFibre, Euralis (Cazeres, France) with the commercial name Cannhabitat®.

The major and trace elements of limes, clay and sand were analysed by means of a S4 PIONEER-BRUKER X-ray fluorescence (XRF) spectrometer with wavelength dispersion, equipped with Rh X-ray tube (60 kV, 150 mA) and LIF200/PET/OVO-55 crystals. Samples were grinded and the powder dispersed in KBr pellets before the analysis.

The identification and semi-quantification of mineral phases of limes, clayey earth and sand was performed by X-ray diffraction (XRD). Limes and sand were analysed using a Panalytical X'Pert PRO MPD diffractometer, with automatic loader, at the following experimental conditions: CuKα radiation (λ ≈ 1.5405 Å); 45 kV voltage and 40 mA current intensity; 3–70° 2θ explored area; 0.01° 2θ/s goniometer speed. To analyse the mineralogy of the clay fraction (below 2 μm) in the earth, the following treatments were carried out: grinding of 100 g of sample left in deionised water; addition of acetic acid (CH_3COOH, 1 N) to eliminate carbonates; washing several times in water to eliminate the acid; addition of hydrogen peroxide (H_2O_2, at 20% by vol.) to eliminate any possible organic matter; addition of sodium hexametaphosphate to separate agglomerates; removal of the excess water; separation of the fraction below 2 μm by means of a Kubota KS-8000 centrifuge. Once the clay fraction was obtained, it was deposited on glass sample-holders using the oriented aggregate method. The oriented aggregates were then treated according to different methods: dissolution in ethylene-glycol for 48 h at 60 °C, to determine the presence of swellable clays [15]; dissolution in dimethyl-sulfoxide for 72 h at 80 °C, to identify the kaolinite phase [16]; heating at 550 °C for 90 min to check the presence of chlorite [17]. Each oriented aggregate was finally analysed using a Philips X'Pert PRO diffractometer at the following working conditions: CuKα radiation (λ ≈ 1.5405 Å); 45 kV voltage and 40 mA current intensity; 3–30° 2 θ explored area; 0.1 2θ/s goniometer speed. The X-ray diffraction patterns were interpreted using the XPowder© software [18].

2.2. Hemp concrete blocks and lime renders

2.2.1. Mixing and compaction

Four types of hemp concrete were prepared to fabricate the blocks: *nlb-L*, blocks for non-load-bearing applications with lime; *lb-L*, blocks for load-bearing applications with lime; *nlb-LC*, blocks for non-load-bearing applications with lime and clay; *lb-LC*, blocks for load-bearing applications with lime and clay. Blocks with sand were named "load-bearing" because the aggregate confers a solid skeleton to the concrete, with consequent increased density and improved mechanical resistances, even though the latter have not been studied here. Mixing of the raw materials was performed in an automatic mixer (Fig. 2a); the concrete was then poured in a mould of 30 × 30 × 30 cm^3, made with four panels of non-absorbent wood, and it was compacted in layers of 10 cm with an iron tool (Fig. 2b). Blocks were left with only one face (Fig. 2c) exposed to the environmental conditions, whilst the opposite face was covered with plastic foils to prevent drying from it (Fig. 2d).

The components, dosages and names of the fabricated blocks are detailed in Table 1.

2.2.2. Curing

Blocks were let dry in absence of ventilation at T = 18 °C and RH = 95% during the first week and at T = 20 °C and RH = 60% from the second week onward. The initially high relative humidity was set to favour the hydration reaction of calcium silicates in the hydraulic lime during the early-age period [7]; one week later, relative humidity was set at 60% to favour carbonation of $Ca(OH)_2$ in the hydraulic lime [19]. This relative humidity is still higher than the average values indicated in literature for an ideal drying of hemp concrete blocks (RH = 45–50% with air convection [7,20].

2.2.3. Rendering

For each block type two different renders 1.2 cm thick were applied, one made with NHL3.5 + natural crushed sand, and the other made with CL90S-PL + natural crushed sand (Table 1). Rendering was performed 2 and 10 weeks after block fabrication, on the face exposed to environmental conditions (Fig. 2e). Two weeks after the block production, the surface of the blocks was still wet, as water drops could be observed especially on the blocks made with earth. For this reason, the surface was not wetted before the render application performed at 2 weeks. Rendering at 10 weeks, instead, was performed after wetting the surface of the blocks with 100 mL of water, by means of a brush.

2.2.4. Control samples

Right after their preparation, control samples were also obtained from each mixture of the hemp concretes and the lime renders, casting them in moulds of 4 × 4 × 16 cm^3 and 10 × 10 × 1.5 cm^3, respectively. The hemp concrete control samples were removed from the mould one week after their casting and they were cured for 6 months at the same conditions as the blocks during the first week (T = 18 °C and RH = 95%), so as to promote a similar drying than in the blocks. The weight loss of the concrete control samples was monitored for the first 3 weeks to test their drying time.

2.3. The study of hemp concretes, lime renders and control samples

Six months after the fabrication of the blocks, photos were taken and samples from the blocks and the lime renders were collected.

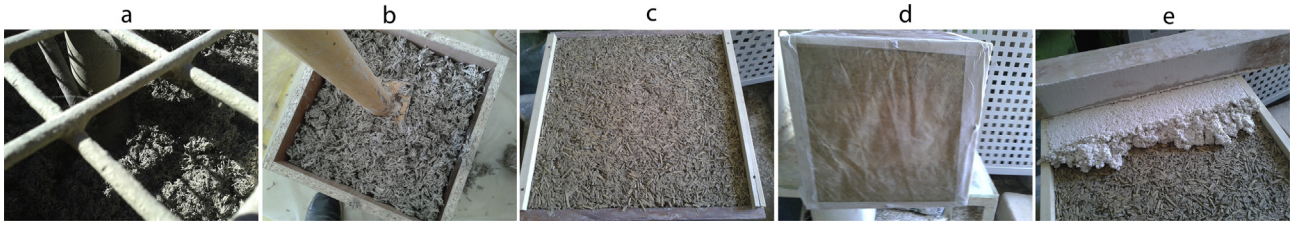

Fig. 2. Steps of the block fabrication: (a) mixing of the components; (b) compaction after pouring; (c) face of the block left exposed to the environmental conditions; (d) opposite face of the block covered with plastic foil; (e) rendering of the exposed surface.

Table 1
Names of the blocks, components and dosages (by volume) of the hemp concrete blocks and the lime renders.

Block name	Hemp concrete components and dosages					Render components and dosages				Rendering time (weeks)
	Hemp shiv	Grey NHL3.5	Clay	Sand	Water	White NHL3.5	CL90S-PL	Sand	Water	
nlb-L_CL_2w	5	2	–	–	1.75	–	1	3	–	2
nlb-L_CL_10w	5	2	–	–	1.75	–	1	3	–	10
nlb-L_NHL_2w	5	2	–	–	1.75	1	–	4	1	2
nlb-L_NHL_10w	5	2	–	–	1.75	1	–	4	1	10
lb-L_CL_2w	4	2	–	1	1.5	–	1	3	–	2
lb-L_CL_10w	4	2	–	1	1.5	–	1	3	–	10
lb-L_NHL_2w	4	2	–	1	1.5	1	–	4	1	2
lb-L_NHL_10w	4	2	–	1	1.5	1	–	4	1	10
nlb-LC_CL_2w	5	1.25	2.5	–	2	–	1	3	–	2
nlb-LC_CL_10w	5	1.25	2.5	–	2	–	1	3	–	10
nlb-LC_NHL_2w	5	1.25	2.5	–	2	1	–	4	1	2
nlb-LC_NHL_10w	5	1.25	2.5	–	2	1	–	4	1	10
lb-LC_CL_2w	5	1.25	3.5	0.5	2.25	–	1	3	–	2
lb-LC_CL_10w	5	1.25	3.5	0.5	2.25	–	1	3	–	10
lb-LC_NHL_2w	5	1.25	3.5	0.5	2.25	1	–	4	1	2
lb-LC_NHL_10w	5	1.25	3.5	0.5	2.25	1	–	4	1	10

The pore system of samples was studied by means of mercury intrusion porosimetry (MIP), using a Quantachrome Poremaster 60 porosimeter, which was useful to determine the interparticle porosity (P_{ip}, in %) of the block control samples, and a Micrometics Autopore III 9410 porosimeter, which was used to determine the open porosity (P_o, in %) and pore size distribution (PSD) of the render samples. Sample fragments of ca. 1 cm^3 were oven-dried for 24 h at 60 °C before the analysis.

XRD analyses were performed on the hemp blocks and the renders, the latter collected both from the blocks and the control samples, using the same methodology described above for the characterization of limes and sand.

The microstructure and morphology of both the hemp concretes (those without sand) and the renders were observed by means of environmental scanning electron microscopy (ESEM), by using a Philips Quanta 400 microscope with a solid state detector (SSD) that works with backscattered electrons. Before observation, the microscope chamber was purged 5 times at a range of pressures between 0.08 and 1 torr. Once equilibrium was achieved, pressure was fixed at 0.5 torr, which is the optimal pressure for an optimised charge and a good backscattered electrons image. Small pieces of samples (~5 mm) were dried before observations.

The chromatic differences between the renders, according to their composition and application time, were detected by means of a portable Konica-Minolta CM-700d spectrophotometer, which measures L^* (lightness), a^* and b^* (chromatism) parameters [21]. Five measurements per sample were performed at the following conditions: measurement area of 8 mm, D65 standard illuminant and observer 10° with modes SCI/SCE and a wavelength range from 400 nm to 700 nm with a wavelength interval of 10 nm. The overall colour difference (ΔE) of the lime renders compared to the control samples was determined as follows: $\Delta E = \sqrt{\left((L_1^* - L_2^*)^2 + (a_1^* - a_2^*)^2 + (b_1^* - b_2^*)^2\right)}$, where L_1^*, a_1^* and b_1^* are respectively the lightness and the chromatic coordinates of the render control samples and L_2^*, a_2^* and b_2^* are those of the renders collected from the blocks.

The surface of the renders (both from the control samples and from the blocks) was observed by means of a Philips Quanta 400 environmental scanning electron microscope (ESEM), which worked with backscattered electrons at a fixed temperature of 2 °C and 3.5 torr (RH ~ 70%). This microscopic technique did not require prior preparation of samples.

A microbiological study was performed on the hemp concrete and the renders from the blocks.

3. Results

3.1. Raw materials

Table 2 shows the chemical and mineralogical composition of the limes, clayey earth and sand. Both limes are clearly rich in CaO, especially CL90S-PL (lime putty), which is almost totally composed of this compound (98 wt%). In NHL3.5, CaO represents about 70 wt% and SiO2 highlights with a 12 wt%. Mg, Al and Fe are other minor components of this lime. The clayey material from Guadix is rich in silica (about 40 wt%) and alumina (~19 wt%) and shows important amounts of calcium and iron. The loss on ignition (LOI) is the highest among the samples studied. The sand has a typical calcitic composition as revealed by the high CaO content (76 wt%), a value that is accompanied by a high LOI content. The content in the other elements is negligible.

In regard to the mineralogical composition, the two limes are different since CL90S-PL is only composed by portlandite (plus traces of calcite that proceeds from an incipient carbonation of portlandite during manipulation of sample for XRD analysis), whilst NHL 3.5, due its hydraulic nature, shows high concentrations of di-calcium and tri-calcium silicates and lower amounts of calcite and portlandite. These differences correspond to the different chemistry just observed. The clayey earth is rich in quartz and phyllosilicates (mainly illite and lower amount of paragonite, chlorite, kaolinite and trace of smectites). Finally, the sand is composed of calcite, as found by XRF.

3.2. Hemp concrete control samples and blocks

3.2.1. Drying process and inter-particle porosity

The drying curves of the hemp concrete control samples are shown in Fig. 3a. After two weeks, non-load-bearing hemp concretes (*nlb–*) lost between 26 and 31% of water whilst load-bearing ones (*lb–*) only lost a 16–22%. Water evaporation was slower in the concretes with sand for a twofold reason: the absorption ability of the calcareous sand (it can retain water in its pores) and the higher density and lower porosity of the load-bearing samples [8]. MIP investigations showed indeed that concrete control samples made with sand have lower interparticle porosity (P_{ip} = 10–12%) than samples made without sand (P_{ip} = 17–18%). The linear trend obtained by plotting the bulk density and the weight of concrete samples at different drying times (Fig. 3b) demonstrates that the weight loss due to drying is proportional to concrete density. Hemp concretes made with lime have the highest and the

Table 2
Chemical (by means of X-ray fluorescence, XRF) and mineralogical composition (by means of X-ray diffraction, XRD) of: grey natural hydraulic lime (NHL 3.5); lime putty (CL90S-PL); clayey earth (clay); natural crushed sand (sand). LOI = loss on ignition; C_2S = di-calcium and tri-calcium silicates; Por = portlandite; Cal = calcite; Qtz = quartz; Ilt = illite; Pg = paragonite; Chl = chlorite; Kln = kaolinite; Fsp = feldspar; Sme = smectite; Dol = dolomite. ****: more than 90%; ***: between 40 and 50%; **: between 20 and 25%; *: between 8 and 12%; *tr*: between 1 and 5%, –: 0%.

Sample	NHL 3.5	CL90S-PL	clay	sand
Chemical composition (XRF) wt %				
Na_2O	0.059	0.008	0.904	–
MgO	3.077	0.697	1.756	0.841
Al_2O_3	2.137	0.151	18.776	0.293
SiO_2	12.347	0.279	39.64	0.697
CaO	69.722	98.247	6.122	76.19
Fe_2O_3	1.175	0.088	6.509	0.185
K_2O	0.578	0.012	3.136	0.046
P_2O_5	0.053	0.042	0.201	0.022
TiO_2	0.127	0.013	0.610	0.020
LOI	9.36	0.20	21.94	21.62
ppm				
S	4540	839	380	
Cl	24	123	42	
Mineralogical composition (XRD) wt. %				
CS	***	–	–	–
Por	**	****	–	–
Cal	**	tr	*	****
Qtz	tr	–	**	–
Ilt	–	–	**	–
Pg	–	–	*	–
Chl	–	–	*	–
Kln	–	–	*	–
Fsp	–	–	*	–
Sme	–	–	tr	–
Dol	–	–	–	tr

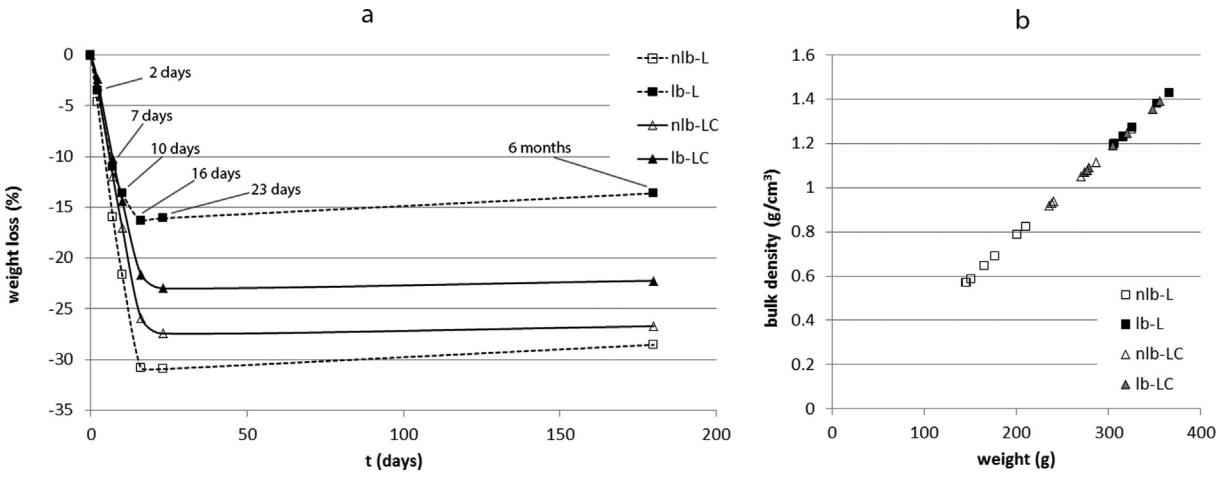

Fig. 3. Hemp concrete control samples cured for 6 months under T = 18 °C and RH = 95%: (a) drying curves where the weight loss (in %) is represented as a function of time (in days); (b) linear correlation between the bulk density (in g/cm^3) and the weight (in g) of concrete during curing. Legend: *nlb-L*, non-load-bearing blocks with lime; *lb-L*, load-bearing blocks with lime; *nlb-LC*, non-load-bearing blocks with clay and lime; *lb-LC*, load-bearing type blocks with clay and lime.

lowest density among concretes, with (*lb-L*) and without sand (*nlb-L*) added, respectively.

This difference is reflected in their drying curves, where non-load-bearing samples lost 31% of their initial wet weight (*nlb-L*, Fig. 3a) whilst load-bearing ones lost only half of this water content (the loss of *lb-L* was 16%, Fig. 3a). In the hemp concretes made with clay and lime, instead, the addition of sand has caused a decrease of the water loss by only 4% (*nlb-LC* lost 26% and *lb-LC* lost 22% of the initial wet weight, Fig. 3a).

3.2.2. Mineral phases and hardening

From the amounts of the mineral phases found in the hemp concrete blocks by means of XRD, it was possible to estimate the carbonation and hydration degrees of the samples, indicated by the hardening index (I, in %) in Fig. 4. There is not a clear relationship between the carbonation or hydration degree of the blocks and the lime type and rendering time. However, from this graph we can draw that applying a coating on the hemp concrete blocks with lime (nlb_L and lb_L) after only 2 weeks limits the carbonation process, especially when the render is made with lime putty (_CL0_2w and _CL_10w). In blocks made with clay, carbonation does not seem to be affected by rendering as much as the hydration process. In general, rendering after 2 weeks seems to be detrimental to the hardening of the lime in the blocks.

In order to understand why carbonation is slowed down in the blocks made with lime and rendered with lime putty, we investigated the differences in the amounts of the carbonation products calcite, vaterite and aragonite, the three polymorphs of calcium carbonate that have all been found by XRD in the blocks made with only lime (nlb_L and lb_L). Differences in their amounts are visible

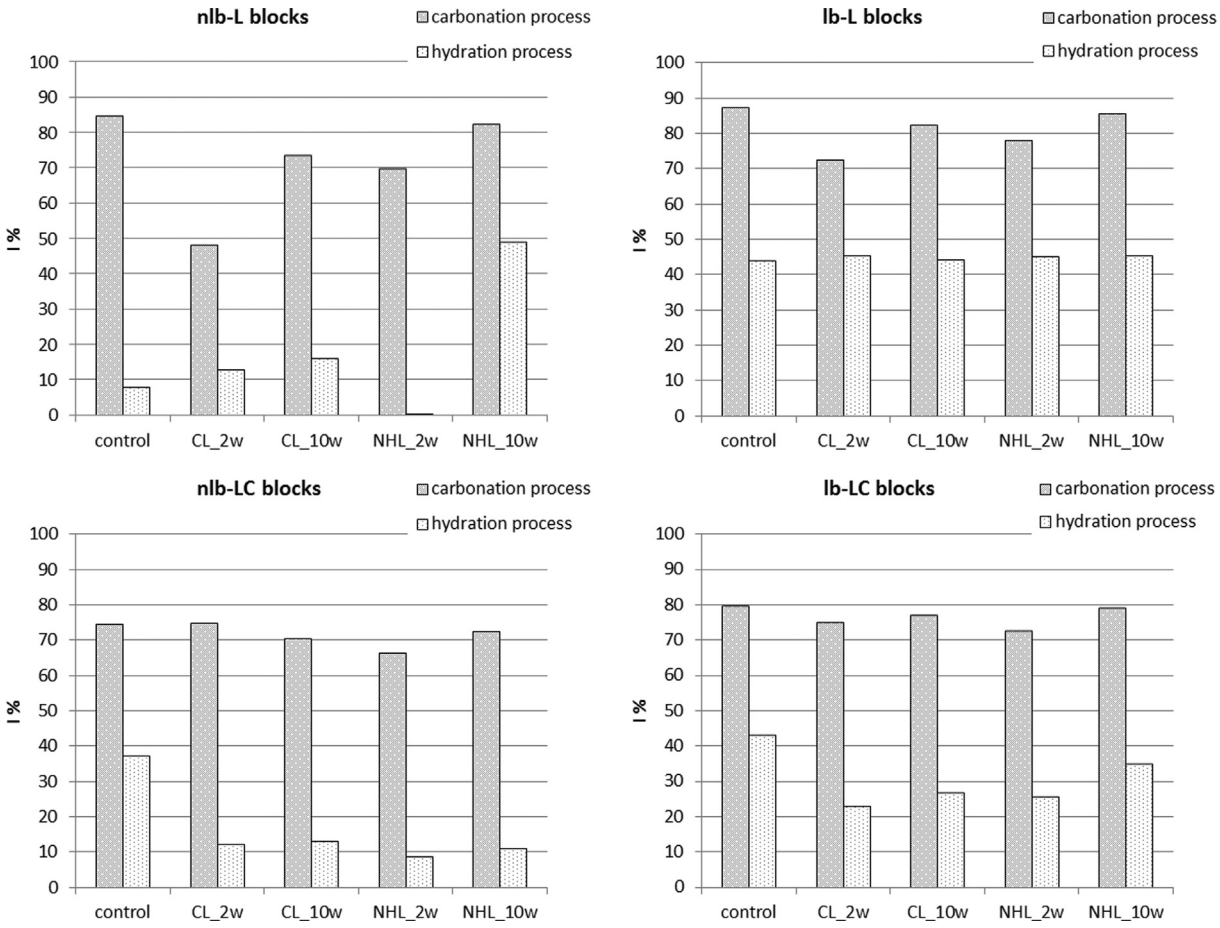

Fig. 4. Hardening index (I, in %) of the hemp concretes taken from the control samples and from the blocks after 6 months of curing. Legend: *nlb-L*, non-load-bearing blocks with lime; *lb-L*, load-bearing blocks with lime; *nlb-LC*, non-load-bearing blocks with lime and clay; *lb-LC*, load-bearing blocks with clay and lime; rendered with CL (CL90S-PL) and NHL (grey NHL3.5) after two (2w) and ten (10w) weeks.

between the hemp concrete control samples (nlb_ and lb_BLANK) and the samples taken from the blocks after rendering with lime putty at 2 and 10 weeks (_2w and _10w, respectively). Calcite is the predominant phase followed by vaterite (around 80% and 20% of the carbonation products, respectively, in nlb-L_BLANK) whilst aragonite has not been detected by XRD in the control blocks. In samples taken from the blocks rendered after 2 weeks, calcite is still the predominant phase (around 80% of the carbonation products in nlb-L_2w), but the vaterite amount decreases considerably (around 9% of the carbonation products in nlb-L_2w) and aragonite can now be detected in small amounts (around 9% of the carbonation products in nlb-L_2w) by XRD. Samples taken from the blocks that were rendered after 10 weeks are similar to the control block samples: calcite is again the predominant phase (around 80% of the carbonation products in nlb-L_10w), whilst vaterite and aragonite amounts are around 15% and 5% of the carbonation products of nlb-L_10w, respectively.

Based on the needle-like morphology of calcium carbonate crystals with sizes of up to 100 μm (Fig. 5) observed by means of ESEM, we could identify aragonite in nlb-L sample.

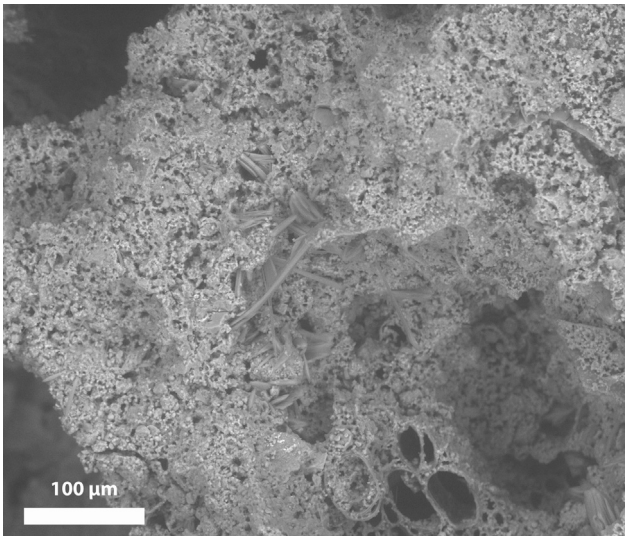

Fig. 5. ESEM image of a small area of a nlb-L sample in which aragonite needle-like crystals can be observed.

3.3. Lime renders

3.3.1. Chromatic changes

The colour differences observed and the chromatic parameters measured after six months on the render control samples and the renders collected from the blocks are shown in Fig. 6.

A colour difference between the CL and the NHL renders was already observed one week after the first rendering (*2w*): CL renders, especially those applied on the blocks made with lime

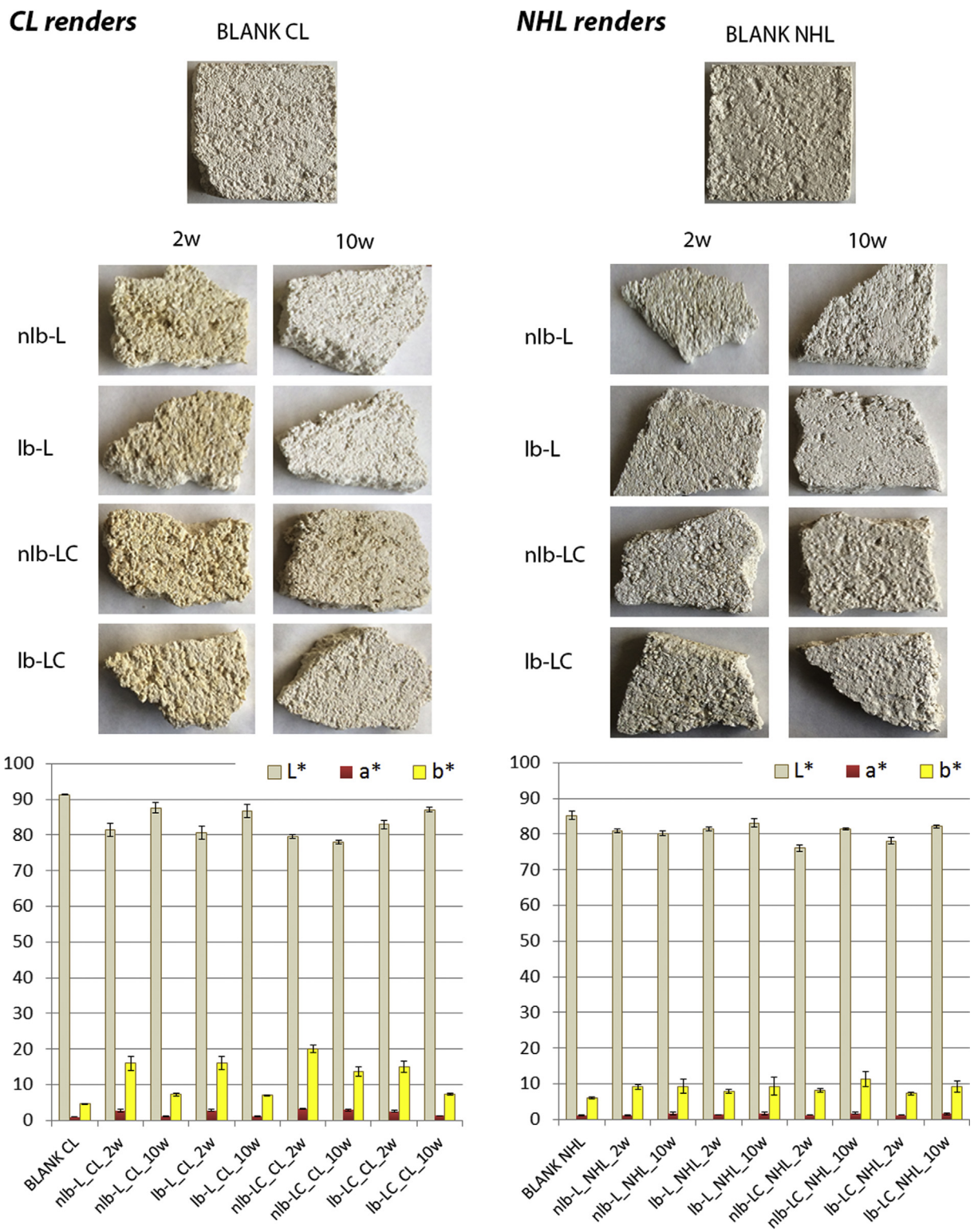

Fig. 6. Photos and chromatic parameters (L^*, a^* and b^*, with error bars) of the *CL* (made with CL90S-PL) and *NHL* (made with grey NHL3.5) control samples (*BLANK CL* and *BLANK NHL*) and the render samples applied after two (2w) and ten (10w) weeks and collected from the blocks after six months (*nlb-L*, non-load-bearing blocks with lime; *lb-L*, load-bearing blocks with lime; *nlb-LC*, non-load-bearing blocks with clay and lime; *lb-LC*, load-bearing blocks with clay and lime).

(*nlb-L* and *lb-L_CL*), acquired a yellowish colour whilst NHL renders were still maintaining their colour after the same period of time. After six months, all the CL renders showed a yellowish colour, except for the renders applied after ten weeks on the blocks made with lime (*nlb-L* and *lb-L_CL_10w*). The NHL renders, instead, did not show any visible colour change, compared to the control sample. However, the human eye hardly detects slight colour changes, reason why it was fundamental to assess the chromatic parameters of all renders by means of a spectrophotometer. According to the graphs shown in Fig. 6, the lightness (L^*) value

decreases by 4–12% in CL renders and by 2–7% in NHL ones, compared to the control samples. The a^* parameter also increases in all samples by 3–15% in CL renders and by 2–5% in NHL ones, as reflected in the more intense yellowing of the CL render surfaces. The b^* parameter, instead, increases only slightly (by 0–2% in CL renders and by 0.2–0.7% in NHL ones). In summary, the highest overall colour difference was found in all CL renders applied after 2 weeks ($\Delta E \sim 15$–20, Table 3) and in the one applied after 10 weeks on the non-load-bearing block made with clay and lime (*nlb-LC_CL_10w*, $\Delta E \sim 13$, Table 3). The colour of NHL renders remained almost unvaried ($\Delta E \sim 4$–6, Table 3), except for a slightly higher chromatic change measured on the renders applied after 2 weeks on the blocks made with lime and clay ($\Delta E \sim 7$–9).

3.3.2. Microbial growth

Table 3 shows the bacteria and fungi isolated in the render control samples and the render samples taken from the blocks.

In CL_BLANK we found two types of Gram positive cocci (*Staphylococcus* and capsulated diplococci) that were also found in lb-LC_CL_10w, whilst in lb-L_CL_10w bacilli were found instead of cocci.

In the renders collected from the blocks we isolated the same fungi than in the render control samples, except for *Aspergillus versicolor* that was only found in the CL_BLANK and yeast that only appeared in nlb-LC_CL_10w sample.

In NHL_BLANK only fungi were isolated (two different species of *Penicillium* and one of *Cladosporium*). The same fungi, except for *Penicillium chrysogenum*, have been isolated in the renders collected from the blocks although a new non-identified species appeared in *nlb-L_NHL_2w* and *nlb-L_NHL_10w* samples. This fungus was not identified because it lacked of reproductive structures (we could only observe hyphae).

Several types of bacteria were isolated in the NHL renders collected from the blocks: 5 types of Gram positive cocci, 2 streptococci and 3 types of Gram positive bacilli.

The majority of isolated microorganisms coincide with those identified in a previous study on the durability of hemp-lime mixes submitted to different weathering conditions [22].

3.3.3. Mineral phases and hardening

The hardening of mortars made with lime putty (CL renders) occurs only through carbonation of the lime; in the hydraulic mortars (NHL renders), instead, hardening is the sum of two processes: carbonation and hydration. Hydration (i.e. reaction of the calcium silicates with water to obtain calcium silicate hydrates) occurs at early-ages (during the first hours or days), therefore it is expected to be completed after six months. Carbonation (i.e. transformation of portlandite into calcite after reaction with atmospheric CO_2) is a slower process that can still be incomplete after several years, although around 80% of the lime is expected to be transformed into calcite after six months [23]. The identification of the mineral phases and the comparison of the height of the peaks in the XRD patterns of the control and collected sample renders (Fig. 7) is a valid method to assess the hardening of the renders and to investigate possible deviations from the expected trend explained above.

The control samples are almost totally hardened, as demonstrated by the absence of portlandite (Por) and calcium silicate peaks (C_2S and C_3S) in the XRD patterns of BLANK CL and BLANK NHL samples. The collected samples, instead, still present low amounts of these two phases, indicating that the renders applied on the blocks hardened slower than expected. The slowest hardening occurred in the two weeks-renders, especially those applied on the non-load-bearing blocks made with clay and lime.

No evidence of the presence of aragonite was found by means of XRD but this phase was observed by means of ESEM, possibly because its content is under the resolution power of the XRD technique. In particular, clusters of big aragonite crystals (with the same morphology as those described in [24] and sizes from 30 up to 200 μm, Fig. 8a) were found in localised areas that correspond to darker spots (Fig. 8b and c), which are likely to be the extracellular polymeric substances (EPS) produced by microorganisms. The biochemical composition of EPS is known to influence the precipitation of carbonate polymorphs, being the acidic proteins isolated in extracellular polymeric substances the ones inducing aragonite formation [25].

Calcite was also observed in the lime putty renders by means of ESEM, and identified on the basis of its morphology as scalenohe-

Table 3
Overall colour difference (ΔE) between the renders from the control samples and from the blocks, and the isolated microorganisms.

Render control samples	bacteria		fungi
CL_BLANK	Gram positive cocci (*Staphylococcus* and capsulated diplococci)		*Aspergillus versicolor; Aspergillus nidulans; Penicillium sp*
NHL_BLANK	-		*Penicillium sp; Penicillium chrysogenum; Cladosporium*
Renders from the blocks	ΔE	bacteria	fungi
nlb-L_CL_2w	15.23	–	–
nlb-L_CL_10w	4.47	–	–
lb-L_CL_2w	15.64	–	–
lb-L_CL_10w	5.08	Gram positive bacilli	*Penicillium sp , Aspergillus nidulans*
nlb-LC_CL_2w	19.51	–	*Penicillium sp*; *Aspergillus nidulans*
nlb-LC_CL_10w	16.26	–	*Penicillium* sp and yeast
lb-LC_CL_2w	13.48	–	*Aspergillus nidulans*; *Penicillium sp*
lb-LC_CL_10w	5.08	Gram positive cocci (*Staphylococcus and* capsulated diplococci)	–
nlb-L_NHL_2w	5.28	Endospores forming bacilli, Gram positive cocci (capsulated diplococci and streptococci)	1 not identified
nlb-L_NHL_10w	5.93	–	1 not identified; *Cladosporium; Penicillium sp*
lb-L_NHL_2w	4.24	Gram positive cocci (*Staphylococcus*)	*Penicillium sp*
lb-L_NHL_10w	3.85	–	*Penicillium sp*
nlb-LC_NHL_2w	9.42	–	–
nlb-LC_NHL_10w	6.46	Gram positive cocci (*Micrococcus*, capsulated diplococci , and estreptococci)	–
lb-LC_NHL_2w	7.26	Gram positive cocci	–
lb-LC_NHL_10w	4.38	Gram positive bacilli (two different species) and Gram positive cocci	–

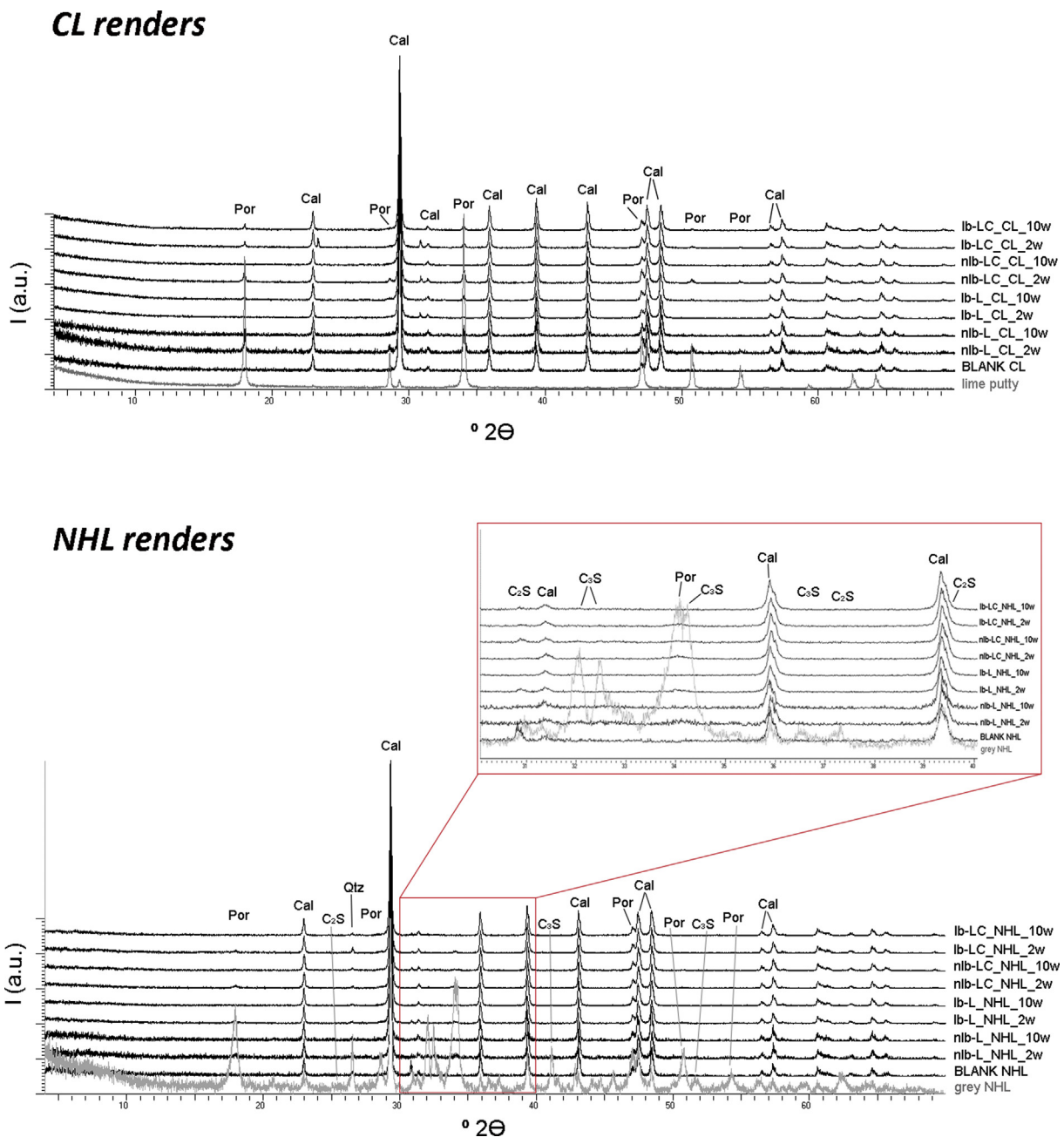

Fig. 7. X-ray diffraction (XRD) patterns of the CL (a) and NHL (b) renders. Legend: lime putty, CL90S-PL; grey NHL, NHL3.5; BLANK CL, CL render control sample; BLANK NHL, NHL render control sample; *nlb-L*, non-load-bearing blocks with lime; *lb-L*, load-bearing blocks with lime; *nlb-LC*, non-load-bearing blocks with clay and lime; *lb-LC*, load-bearing blocks with clay and lime; *CL_2w*, rendered with CL90S-PL after 2 weeks; *CL_10w*, rendered with CL90S-PL after 10 weeks; *NHL_2w*, rendered with grey NHL3.5 after 2 weeks; *NHL_10w*, rendered with grey NHL3.5 after 10 weeks. Por: portlandite; Cal: calcite; C_2S: di-calcium silicate; C_3S: tri-calcium silicate; Qtz: quartz.

dral and rhomboedral-like particles, respectively (Fig. 8d and e). In the NHL renders the typical needle-like morphology of the calcium silicate hydrated (CSH) phases was also identified (Fig. 8f).

4. Discussion of the results

Studying the drying kinetics of the hemp concrete control samples was helpful to predict the drying trend of the blocks, even though the exposure conditions were slightly different after the first week. On the basis of our results, we expect that a faster drying occurs in the non-load bearing blocks, especially those made with only lime.

According to Colinart et al. [7] drying of compacted hemp concretes occurs in three main stages: firstly, water in the liquid state migrates towards the surface; secondly, water is trapped in the pores of the material close to the surface; finally, water is slowly removed through vapour transport.

The fact that non-load-bearing blocks dried faster than the other blocks means that a greater amount of water could have migrated towards the exposed surface in the same period of time (2 weeks). This suggests that when the blocks made with lime were coated with a render after two weeks, they were drier than the blocks made with clay and lime. Therefore in the latter more water is likely to have been trapped underneath the render, creating an area with high relative humidity that would have favoured

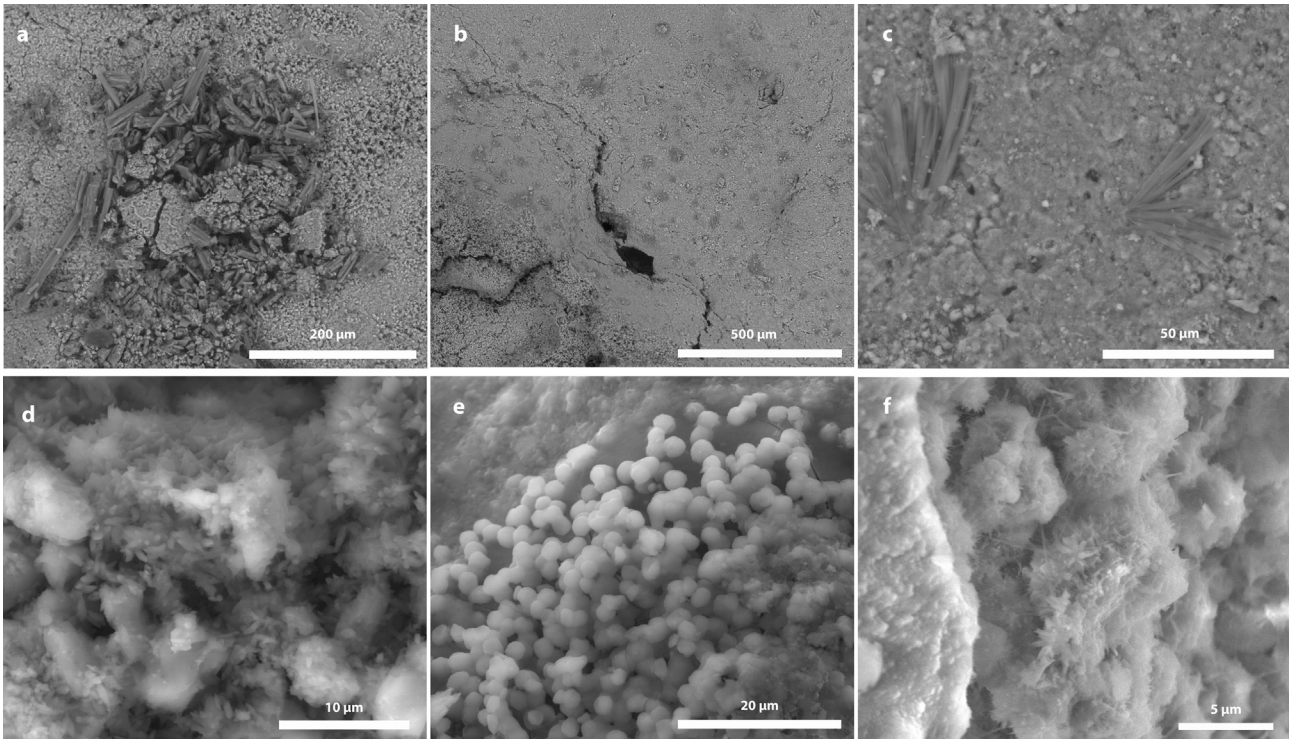

Fig. 8. ESEM images of the mineral phases formed in renders: aragonite crystals in CL render applied on nlb-L (a) and lb-LC (b and c) blocks; scalenohedral calcite in CL render applied on nlb-L block (d); rhomboedral calcite in CL render applied on lb-LC block (e); needles of CSH in NHL render applied on nlb-L block (f). The square in (b) is the magnified area shown in (c).

mould formation, as suggested by Colinart et al. [7]. The presence of a high humidity underneath the render can also induce swelling of the smectite present in the clayey earth used, with consequent long-term damage of the wall. In addition to this, it is worth highlighting that, during liquid and vapour migration toward the surface, water transports in it all the organic compounds released by the hemp shiv [26,27]. If rendering is performed before the end of the early drying process, these compounds deposit on the render, causing pigmentation and microbial colonisation of the surface. This indeed occurred in the 2-weeks-rendered samples more than in the 10-weeks-rendered ones. Moreover, a more intense pigmentation was observed in the render samples collected from the blocks made with clay and lime, as they dried slower, regardless the type of render applied. It is worth highlighting that the iron content in the clayey earth used can also be responsible of the pigmentation of the surface of renders, due to the possible crystallisation of little amounts of iron oxides and hydroxides.

The hardening of the render itself is conditioned by the drying of the blocks, being slower in renders made with lime putty and applied on the blocks made with clay and lime. This is consistent with the fact that carbonation is slowed down when the water content in the pores is higher than 50% [17]: being the render more humid due to the higher water content underneath it, the diffusion of CO_2 through the pore system is slowed down, and less carbonated products are formed as a consequence. On the one hand, the precipitation of aragonite could be an evidence of the higher relative humidity of the renders made with lime putty and applied on the load-bearing blocks. López-Arce et al. [28] found, indeed, that aragonite is formed from calcium hydroxide nanoparticles exposed to high RH (75–90%). On the other hand, the aragonite formation has also to be linked to the presence of EPS [29], according to our ESEM observations.

5. Conclusions

The performances of non-load bearing and load-bearing hemp concrete made with lime or with clay and lime and the pathologies arisen on renders made with lime putty or natural hydraulic lime when they are applied on it have been investigated here.

When a render is applied on compacted concrete made with hemp composite the following recommendations need to be taken into account:

1) Load-bearing blocks dry slower than non-load bearing ones, due to their higher density (for materials with the same thickness).
2) Adding clay to hemp concrete delays the drying process and cause a more intense pigmentation on the render (due to the iron content in the clayey earth), compared to hemp concrete made with only lime.
3) Under unfavourable conditions of drying (absence of ventilation through all the surfaces) it is advisable to wait a minimum of 3 weeks for the application of a coating since the fabrication of the block. When possible, it would be advisable to wait 10 weeks, so as to ensure the complete drying of the hemp concrete and the correct evolution of the render hardening process.
4) Natural hydraulic lime has to be preferred to aerial (non-hydraulic) lime as binder for rendering rammed earth walls made with hemp concrete. Faster hardening, lower pigmentation and less microbial colonisation are indeed achieved with natural hydraulic lime.

It is worth highlighting that the conclusions drawn in this study are also valid for the application of a plaster, especially with respect to the choice of the binder. However, being the covered

surface of the compacted hemp wall the internal one, its drying time is inevitably longer than that of the external surface, which is exposed to wind and sunlight. This means that more caution about the drying process of the wall is needed when plastering.

Conflict of interest

None.

Acknowledgements

This research was financially supported by: the European Commission under the Marie Curie program (FP7-PEOPLE-2012-IEF call, research project "NaturaLime"); the Spanish Ministry of Economy, Industry and Competitiveness under the program "Juan de la Cierva-Incorporación" (2015 call); the Spanish research project MAT2016-75889-R.

References

[1] M. Pervaiz, M.M. Sain, Carbon storage potential in natural fiber composites, Resour. Conserv. Recyl. 39 (2003) 325–340.
[2] A.M. Esmail, Cannabis Sativa: an optimization study for ROI, Massachusetts Inst. Technol. (2010).
[3] O. Faruk, A.K. Bledzki, H.-P. Fink, M. Sain, Biocomposites reinforced with natural fibres: 2000–2010, Prog. Polym. Sci. 37 (2012) 1552–1596.
[4] R. Bevan, T. Woolley, Hemp lime construction, in: A Guide to Building with Hemp Lime Composites, HIS BRE Press, Bracknell, UK, 2008, pp. 41–42.
[5] A.D. Tran Le, C. Maalouf, T.H. Mai, E. Wurtz, F. Collet, Transient hygrothermal behaviour of a hemp concrete building envelope, Energy Build. 42 (2010) 1797–1806.
[6] M. Brümmer, M.P. Sáez-Pérez, J. Durán Suárez, Hemp Fiber Based Light Weight Concretes For Environmental Building – Parameters that influence the Mechanical Strength, 3rd International Conference on Natural Fibers ICNF 2017, 2017.
[7] T. Colinart, P. Glouannec, P. Chauvelon, Influence of the setting process and the formulation on the drying of hemp concrete, Constr. Build. Mater. 30 (2012) 372–380.
[8] N. Holcroft, A. Shea, Effect of compaction on moisture buffering of hemp-lime insulation, in: S. Amziane, M. Sonebi (Eds.), Proceedings of the 1st International Conference on Bio-Based Building Materials, Charlet K; RILEM Publications S.A.R.L., 2015, pp. 542–546. ISBN PRO 99: 978-2-35158-154-4.
[9] P. Walker, R. Keable, J. Martin, V. Maniatidis, Rammed earth, in: Design and construction guidelines, BRE Bookshop, Watford, UK, 2005, pp. 70–72.
[10] F. Collet, S. Pretot, Experimental highlight of hygrothermal phenomena in hemp concrete wall, Build. Environ. 82 (2014) 459–466.
[11] E. Latif, M. Lawrence, A. Shea, P. Walker, Moisture buffer potential of wall assemblies incorporating hemp-lime, in: S. Amziane, M. Sonebi (Eds.), Proceedings of the 1st International Conference on Bio-Based Building Materials, Charlet K; RILEM Publications S.A.R.L., 2015, pp. 455–459. ISBN PRO 99: 978-2-35158-154-4.
[12] H.R. Kymalainen, A.M. Sjoberg, Flax and hemp fibres as raw materials for thermal insulations, Build. Environ. 43 (2008) 1261–1269.
[13] J.M.P.Q. Delgado, A.S. Guimarães, V.P. Freitas, Air drying technologies applied to building treatment, in: J.M.P.Q. Delgado (Ed.), Drying and wetting of building materials and components. Building Pathology and Rehabilitation, Springer International Publishing, Switzerland, 2014.
[14] EN 459-1. Building Lime. Part 1: Definitions, specifications and conformity criteria. CEN, European Standard, 2010.
[15] G. Bruton, Vapour glycolation, Am. Mineral. 40 (1955) 124–126.
[16] F. González García, M. Sánchez, Camazano, Differentiation of kaolinite from chlorite by treatment with dimethylsulphoxide, Clay Miner. 7 (1968) 447–450.
[17] D.M. Moore, R.C. Reynolds, X-Ray Diffraction and the Identification and Analysis of Clay Minerals, Oxford University Press, Oxford, 1989, p. 322.
[18] J.D. Martín Ramos, XPowder, a software package for powder X-ray diffraction analysis. Lgl. Dep. GR 1001/04, 2004.
[19] D.R. Moorehead, Cementation by the carbonation of hydrated lime, Cem. Concr. Res. 16 (1986) 700–708.
[20] L. Arnaud, E. Gourlay, Experimental study of parameters influencing mechanical properties of hemp concretes, Constr. Build. Mater. 28 (2011) 50–56.
[21] EN 15886, Conservation of cultural property – Test methods – Colour measurement of surfaces, CEN European Standard, 2011
[22] A. Arizzi, H. Viles, I. Martín-Sánchez, G. Cultrone, Predicting the long-term durability of hemp-lime renders in inland and coastal areas using Mediterranean, Tropical and Semi-arid climatic simulations, Sci. Tot. Environ. 542 (2016) 757–770.
[23] A. Arizzi, G. Cultrone, The influence of aggregate texture, morphology and grading on the carbonation of non-hydraulic (aerial) lime-based mortars, Q. J. Eng. Geol. Hydroge. 46 (2013) 507–520.
[24] B. Jones, Review of calcium carbonate polymorph precipitation in spring systems, Sediment. Geol. 353 (2017) 64–75.
[25] T. Kawaguchi, A.W. Decho, A laboratory investigation of cyanobacterial extracellular polymeric secretions (EPS) in influencing $CaCO_3$ polymorphism, J. Cryst. Growth 240 (2002) 230–235.
[26] S. Amziane, L. Arnaud, Bio-Aggregate-Based Building Materials: Applications to Hemp Concretes, Wiley-ISTE, Surrey, UK, 2013.
[27] Y. Diquelou, E. Gourlay, L. Arnaud, B. Kurek, Impact of the hemp shiv on cement setting and hardening: influence of the extracted components from the aggregates and study of the interfaces with the inorganic matrix, Cem. Concr. Compos. 55 (2015) 112–121.
[28] P. López-Arce, L.S. Gómez-Villalba, S. Martínez-Ramírez, M. Álvarez de Buergo, R. Fort, Influence of relative humidity on the carbonation of calcium hydroxide nanoparticles and the formation of calcium polymorphs, Powder Technol. 205 (2011) 263–269.
[29] O.A. Jimoh, K. Shah Ariffin, H. Bin Hussin, A.E. Temitope, Synthesis of precipitated calcium carbonate: a review, Carb. Evap. 1–16 (2017) DOI, https://doi.org/10.1007/s13146-017-0341-x.